Shear Behavior of Ultra High Performance Concrete Beams without Stirrups

Solhmirzaei, R.[1], Kodur, V.K.R.[2], and Banerji, S.[1]

[1]PhD Student, Civil and Environmental Engineering, Michigan State University, East Lansing, MI, USA. Email address: solhmirz@msu.edu

[2] University Distinguished Professor, Department of Civil and Environmental Engineering, Michigan State University, East Lansing, MI, USA. Email address: kodur@egr.msu.edu

Abstract:

Ultra high performance fiber reinforced concrete (UHPC) possesses high compressive and tensile strength, as well as higher ultimate tensile strain, and this can be utilized to realize high shear capacity in UHPC beams. A finite element based numerical model is developed in ABAQUS for tracing response of UHPC beams throughout the loading range; from preloading to collapse stage. The model accounts for detailed stress strain response of UHPC in both compression and tension and strain hardening effect. Response parameters generated from the model namely deflections, crack propagation, and failure mode are validated against measured data from experiments on UHPC beams. The developed model is applied to study the response of beams with varying shear reinforcement ratio to explore the feasibility of eliminating stirrups in UHPC beams. Results indicate that unlike conventional concrete beams, UHPC beams perform well under dominant shear loading even when no stirrups are provided. In other words, eliminating stirrups does not result in reduction of ductility and load carrying capacity of UHPC beams.

Keywords: Ultra high performance concrete, Steel fibers, Shear response, Shear reinforcement, Finite element analysis

1. Introduction

Extensive research and development efforts, over the past three decades, to improve properties of concrete have led to the emergence of Ultra High Performance Concrete (UHPC). In order to improve ductility of UHPC, fibers are often added to UHPC (Ahmed Sbia et al., 2014; Kang et al., 2010). Previous experimental studies on the response of UHPC beams indicate that increasing steel fiber content having relatively high specific surface area (small aspect ratio) in UHPC, enhances post cracking stiffness and thus improves load carrying capacity of UHPC beams (Graybeal, 2008; Yang et al., 2011; Empelmann et al., 2008; Yoo and Yoon, 2015; Solhmirzaei and Kodur, 2018). However, only limited numerical studies are reported on the structural behavior of UHPC beams (Chen and Graybeal, 2011; Mahmud et al., 2013; Singh et al., 2017; Tysmans et al., 2015). These studies focused on flexural response of UHPC beams, and relied on global response of UHPC structural members with no attention to local response (crack propagation).

Despite recent efforts to study structural behavior of UHPC, very limited design guidelines and recommendations exist for designing structural members fabricated using UHPC, with no standard guidelines in the US context. These guidelines need to be developed while giving due consideration to superior mechanical and durability properties of UHPC under different kinds of loading. To evaluate response of UHPC members at structural level, a finite element based numerical model in ABAQUS was developed. The model specifically accounts for superior

strength properties of UHPC, including high compressive strength and tensile strength, strain hardening effect in tension, and bond between UHPC and reinforcing steel.

2. Finite Element Model

A finite element based numerical model for tracing structural behavior of concrete beams under flexural and shear loading, incorporating bond interaction between steel reinforcing bar and concrete, was developed in ABAQUS. A displacement control technique was applied to trace softening behavior of the beams during post peak phase, wherein displacement incremented at the nodes located under load points in steps till failure is attained. This model was applied to study the response of UHPC beams subjected to flexural and shear dominant loading.

2.1. Discretization of the Beam

The UHPC beams were discretized using brick elements with reduced integration (C3D8R). C3D8 element is of eight nodes with three degrees of freedom (available in ABAQUS library). The steel reinforcing bars were modeled using truss elements (T3D2) which are two noded elements (ABAQUS, 2014). Sensitivity analysis indicated that mesh size of 25mm was able to successfully predict post yield response of the beams.

Tension stiffening in concrete is influenced by tensile stress transfer from bar to surrounding concrete through interfacial bond between them. Therefore, in order to have realistic predictions of deflections in beams after tensile cracking, bond-slip between rebar and concrete was modeled to account for effect of tension stiffening. The bond between concrete and reinforcement was modeled by using bond-link element approach (Jendele and Cervenka, 2006; Kodur and Agrawal, 2017) wherein concrete and reinforcing steel were represented by two different sets of elements. At each node pair, three spring elements were modeled with one spring representing slip between reinforcing steel and concrete according to a bond-slip relation (related only to the longitudinal axis direction). The other two springs represented the normal bond behavior in the vertical direction which were assumed to be rigid. The proposed model by Yoo et al. (2014) was utilized to define bond behavior of steel bars embedded in UHPC.

2.2. Material Models for Concrete and Steel

Material models representing stress-strain behavior of UHPC in compression and tension states are needed for undertaking detailed analysis of UHPC structures. While such models are well established for both normal strength concrete (NSC) and high strength concrete (HSC), there are limited relations for tracing uniaxial compressive and tensile stress-strain behavior of UHPC. For this purpose, a material model relating stress strain behavior of UHPC to compressive strength and modulus of elasticity was developed as part of this study.

The uniaxial stress strain response of UHPC can be approximated with a quad-part model including softening branch. A schematic representation of the proposed relation for stress-strain response of UHPC under compression is shown in Figure 1. UHPC under compression exhibits linear behaviour upto almost 70% of its compressive strength (Graybeal, 2007). The linear part of stress strain response is followed by a nonlinear phase until peak strength is reached and can be calculated using a reduction factor (α). This reduction factor (α) defines reduction of stress from linear elastic stress (Graybeal, 2007). For the proposed relations, compressive strength of UHPC (f_c') which varies depending on fiber content and type, curing regime, mix design, etc. is to be

input and this is to be determined through uniaxial compression test. Then, the ascending branch (1-2, 2-3 in Figure 1) of compressive stress strain response is calculated using Equations 1 to 4, where ε, E, f_c', and α are compressive strain, elastic modulus, compressive strength, and reduction factor, respectively.

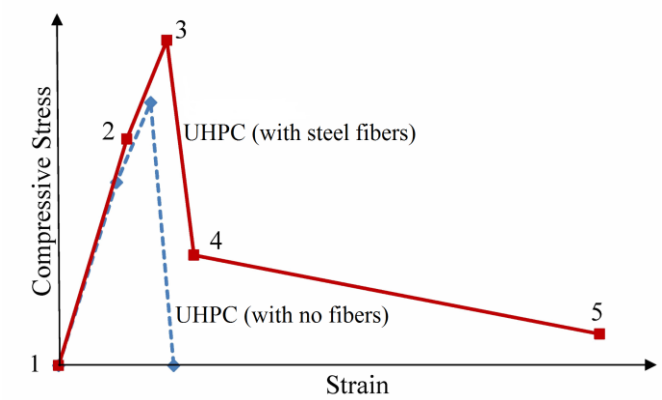

Figure 1. Approximation for compressive stress-strain behavior of UHPC

$$f_c = E\varepsilon \qquad for\ \ 0 < f_c \le 0.70\, f_c' \tag{1}$$

$$f_c = E\varepsilon(1-\alpha) \qquad for\ \ 0.70\, f_c' < f_c \le f_c' \tag{2}$$

$$\alpha = 0.001\, e^{\frac{\varepsilon E}{0.243 f_c'}} \tag{3}$$

Using data from literature, elastic modulus of UHPC was plotted as a function of $(\frac{f'_c}{10})^{(\frac{1}{3})}$ and an empirical model available in literature for calculating elastic modulus of high strength concrete was modified for UHPC as Equation 4. The descending branch (3-4, and 4-5 in Figure 1) is obtained based on empirically derived values from experiments conducted by Empelmann et al (2008). The relations to calculate these five key points based on fiber content and fiber size (aspect ratio) are presented in Table 1. Where ε_0 is the strain corresponding to compressive strength and v_f, l_f, and d_f are fiber volume fraction, fiber length and diameter, respectively. Behavior of UHPC with no fibers is also linear upto 70% of compressive strength and it fails in brittle manner under compression (explosive) (Fehling et al., 2004) as shown in Figure 1.

$$E = 18000\, (\frac{f'_c}{10})^{(\frac{1}{3})} \tag{4}$$

Table 1. Relations for calculating quad part stress-strain approximation of UHPC under compression

Point i	$\varepsilon_i/\varepsilon_0$	f_{ci}/f'_c
1	0	0
2	0.70	(1-α)
3	1	1
4	1.25	$0.35\, v_f l_f/d_f$
5	5	$0.1\, v_f l_f/d_f$

Behavior of UHPC without fibers under tension after cracking is brittle and does not exhibit strain hardening and a significant descending branch as shown in Figure 2(a) (Fehling et al., 2004). However, the fibers present in UHPC induce significant bridging stress between open crack faces leading to high fracture toughness and ductility in UHPC. Therefore, it is essential that this fiber bridging mechanism is effectively incorporated in modeling tensile fracture of UHPC through

stress strain response in tension. Typical stress strain behavior of UHPC in tension is idealized into three stages as shown in Figure 2(a). The initial part is linear elastic upto cracking stress, which is followed by strain hardening part accompanied by initiation of multiple cracking facilitated by fiber bridging. This is further followed by softening branch that represents crack opening with fiber bridging. Tensile behavior of UHPC is influenced by various factors such as characteristic strength of the concrete matrix, fiber type, orientation and distribution of fibers, fiber aspect-ratio and fiber content. The key points of tensile stress strain response, namely cracking, peak, and ultimate points is to be evaluated from direct tension tests. Tensile behavior of UHPC cast for this study (Kodur et al., 2018) as well as UHPC studied by Singh et al (2017) under direct tension is presented in Figure 2(b).

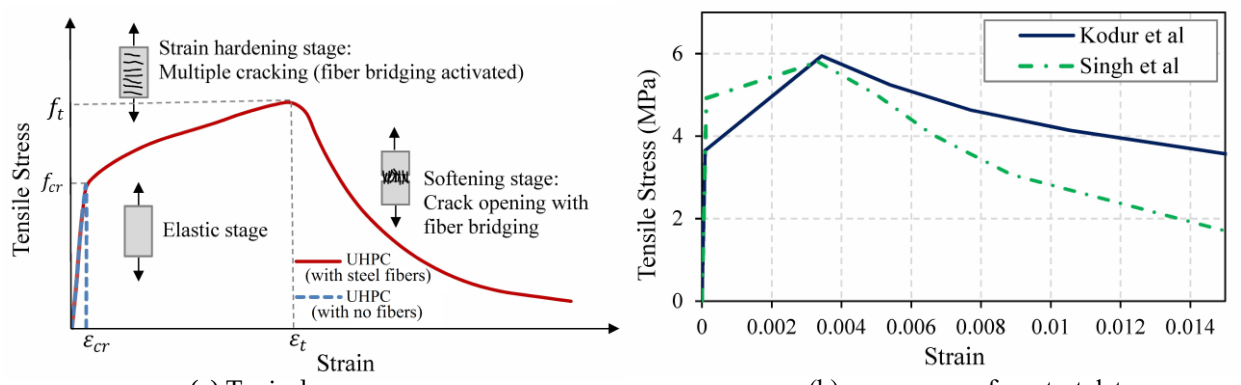

(a) Typical σ-ε response (b) σ-ε response from test data

Figure 2. Tensile stress strain response of UHPC

2.2.1. Concrete Plasticity Model

The above stress strain relations are to be incorporated into a plasticity model to trace behavior of concrete beams. A damage based concrete plasticity model, available in ABAQUS, was utilized to capture the nonlinear material behavior of UHPC. The Concrete Damage Plasticity model (CDP) allows to incorporate strain hardening in compression, strain stiffening in tension, and uncoupled damage initiation and accumulation in tension and compression. In order to define CDP model, material properties including compression response, tension stiffening, elastic modulus, poison ratio, and density needs to be input for analysis. Poison ratio, and density of UHPC were considered to be 0.2, and 2565 kg/m^3 respectively. In addition, the parameters $(\sigma_{b0}/\sigma_{c0}, k_c, \psi, \xi, \mu)$ are required to define CDP model. Parameters σ_{b0}/σ_{c0} and k_c which influences the yield surface in a plane stress state and deviatoric plane were adopted to be 1.05 and 0.67 for UHPC. The other two parameters of dilation angle and eccentricity (ψ, ξ) modifying the non-associated potential flow were assumed to be 30 and 0.1, respectively. μ (viscosity parameter) was selected to be 1E-4 according to sensitivity analysis in this study. In order to account for reduction in stiffness due to cracking, tension damage parameter (Equation 5) was incorporated in the model. The stiffness degradation in compression was also included in the CDP model as Equation 6, wherein σ_t, f_t, σ_c, E, and σ_c are tensile stress, tensile strength, elastic modulus, and compressive stress respectively (Chen and Graybeal, 2011; Singh et al., 2017).

$$d_t = 1 - \frac{\sigma_t}{f_t} \tag{5}$$

$$d_c = 1 - \left[\frac{\sigma_c/E}{0.2\varepsilon_c^{in} + \sigma_c/E}\right] \tag{6}$$

2.2.2. Material Model for Reinforcing bars

A metal plasticity model that utilizes Mises yield surface with associated plastic flow and isotropic hardening available in ABAQUS was adopted for the constitutive modelling of reinforcing steel. The stress strain response of steel reinforcement under tension and compression consisting of three phases of linear elastic, yield plateau, and strain hardening obtained from direct tension test was incorporated in the model.

2.3. Modeling Cracking and Failure

The model is capable of tracing crack propagation zone with increased load by plotting scalar tensile damage parameter. The damage parameter in tension is activated after reaching peak tensile strength and is a function of the plastic strain. Therefore, damage contours replicate tensile cracking and the extent of damage increases with increase in strain at higher load levels (crack widening). In other words, tensile damage parameter of 0 and 1 represent no tension damage and complete damage state, respectively. Direction of cracking and failure mode (shear or flexure) was predicted using direction of principal strain being perpendicular to crack direction.

3. Validation of the Model

The developed finite element model was validated by comparing predicted response parameters with measured data from tests conducted on UHPC beams under flexural and shear loading (Kodur et al., 2018). The beams were designed with no shear and compression reinforcements. These beams were fabricated using UHPC mix with steel fibers of 1.5% volume fraction. The steel fibers were of straight type with 0.2mm diameter and 13mm length. Average compressive strength and elastic modulus of cast UHPC were measured to be 167 MPa and 40615 MPa, respectively. Details of these beam are presented in Table 2 and Figure 3, and additional details regarding experimental program can be found in (Kodur et al., 2018).

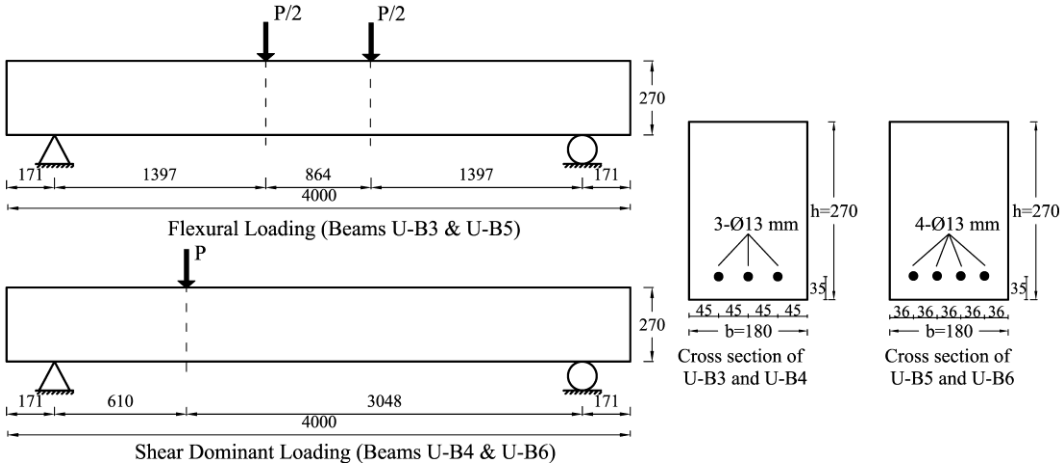

Figure 3. Layout and cross section of UHPC beams used for validation (All dimensions are in mm)

Load-deflection response of UHPC beams as predicted by the model was compared against experimental data in Figure 4. It can be seen that the model was able to predict different stages in response i.e., linear elastic stage until initiation of tensile cracking, post-cracking stage, onset of yielding in steel reinforcement, and plastic deformation stage till peak load followed by attainment of failure. Ratio of total load carrying capacity (P) predicted by the model to that of experimental

results ranges from 0.92 to 0.99 for UHPC beams (see Table 2). However, post cracking response predicted by finite element analysis (FEA) is slightly stiffer than experimental results. This difference can be attributed to possible cracks presented in concrete due to dry shrinkage arising from high dosage of cementitious material and variations arising from material models.

Table 2. Details of beams for validating the model

Beams	Width (mm)	Depth (mm)	Span (mm)	ρ_t (%)	Loading condition	Total load carrying capacity; P (kN)		Ratio of P
						FEA	Test	FEA/Test
U-B3	180	270	3658	0.90	4-point	94.9	97.1	0.98
U-B4	180	270	3658	0.90	3-point	140.1	142.1	0.99
U-B5	180	270	3658	1.20	4-point	117.7	126.6	0.93
U-B6	180	270	3658	1.20	3-point	163.5	177.1	0.92

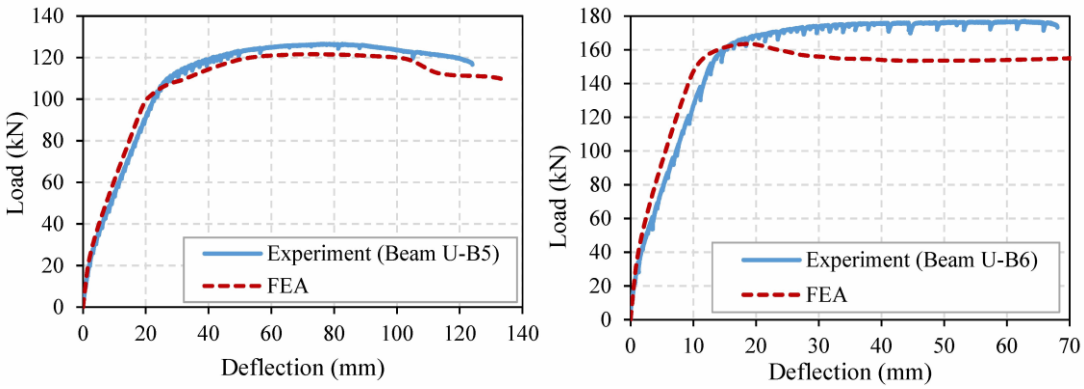

(a) Beam U-B5 (b) Beam U-B6

Figure 4. Comparison of load deflection response of UHPC beams with FEA results

Tensile damage contours and crack direction obtained by FEA at two different states of loading for beams U-B5 and U-B6 (Kodur et al., 2018) along with experimental results are illustrated in Figure 5. In beam U-B5, under flexural loading, tensile damage initiated at extreme tension fibers of the beam in the pure bending zone between load points. Direction of principal strains confirms propagation of flexural cracks. As the load increased further, flexural cracks propagated toward compression zone. The tension damage contours indicate that maximum tension damage at failure is concentrated at critical section of the beam (mid-span) which coincides with the macro crack seen in the experiment. Also, predicted principal direction at failure in Figure 5(a) confirms occurrence of flexural failure.

In the case of beam U-B6, under dominant shear loading, tensile damage initiated at extreme tension fibers confined between point of load application and mid-span due to high levels of tensile stress as shown in Figure 5(b). Principal strains direction indicates that these cracks (between loading point and mid-span) were mainly flexural cracks as observed in the experiment. At increased load levels, shear stresses in shear span significantly increased causing maximum principal stresses to exceed tensile capacity of UHPC. This resulted in significant tensile damage in the shear span. The principal direction in shear span coincides well with diagonal tension crack direction (which is perpendicular to principal direction) seen in the experiment. The tensile damage contour and principal direction shown in Figure 5 agrees well with experiment observations.

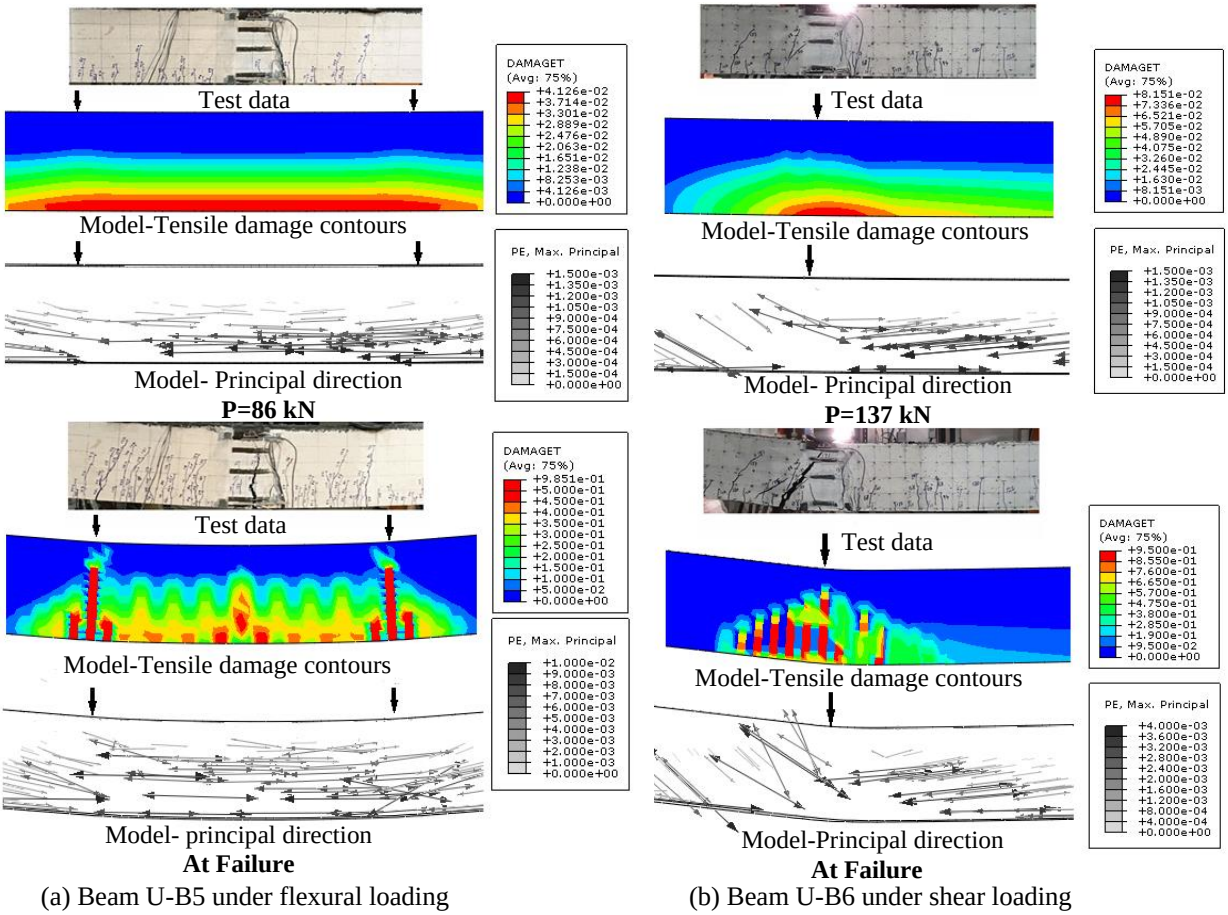

Figure 5. Tensile damage contour and principal strain direction obtained by FEA representing cracks and their direction in beams U-B5 and U-B6 along with test results

4. Effect of Eliminating Stirrups in UHPC Beams

Ultra high performance fiber reinforced concrete possesses high compressive and tensile strength, as well as ultimate tensile strain, and this can be utilized to realize high shear capacity in UHPC beams. With this as one of the objectives, the developed model was utilized to study feasibility of eliminating shear reinforcement in UHPC beams. For this purpose, behavior of tested UHPC beams U-B4 and U-B6 (Kodur et al., 2018) as well as similar NSC beams, with the same cross sectional details, were evaluated under dominant shear loading with different shear reinforcement ratios using developed numerical model. The material model for NSC recommended by ABAQUS documentation (2014) were incorporated into the model. Load deflection response of NSC beams with different longitudinal tensile reinforcement (i.e. ρ_t=0.90% and ρ_t=1.20%) with and without stirrups (ρ_v=0% and ρ_v=0.79%), is shown in Figure 6. As it is shown, eliminating stirrups resulted in reduction of load carrying capacity by almost 15% in NSC beams. Also, NSC beams without shear reinforcement (stirrups), exhibited concrete crushing and significant reduction of stiffness after reaching peak load as compared to NSC beams with stirrups.

In addition, stress distribution along the tensile reinforcement bars in NSC beam (ρ_t=0.90%) with and without stirrups at peak load is shown in Figure 7. The results indicate that reinforcing bars in NSC beam with stirrups yielded, as opposed to NSC beam with no stirrups. In other words the beam with shear reinforcement reached its ultimate moment capacity before failure. However NSC

beam without stirrups failed in shear mode before reaching ultimate moment capacity (and yielding of longitudinal reinforcement).

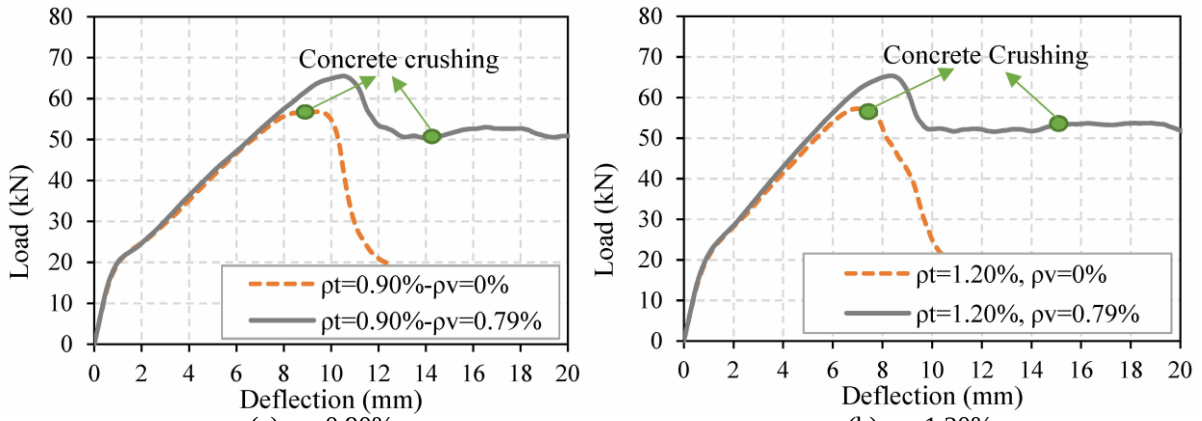

(a) ρ_t=0.90% (b) ρ_t=1.20%

Figure 6. Load deflection response of NSC beams with same cross section as beams U-B4 and U-B6

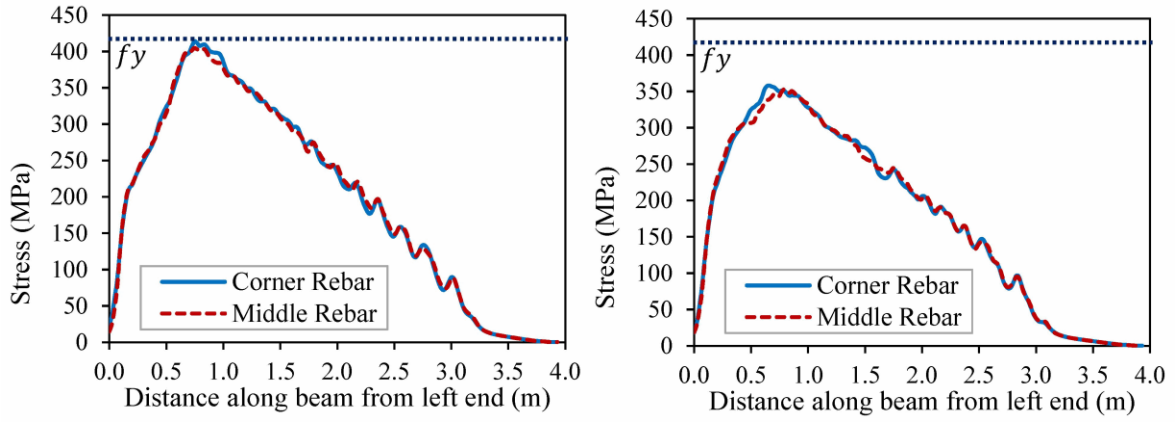

(a) With stirrups (b) With no stirrups

Figure 7. Stress distribution in longitudinal reinforcing bars in NSC beam (ρ_t=0.90%) along the beam length

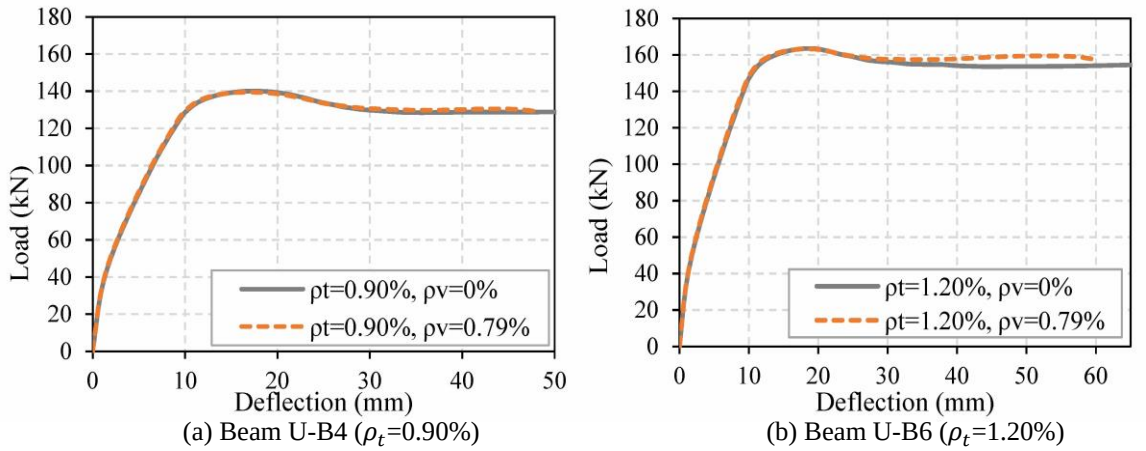

(a) Beam U-B4 (ρ_t=0.90%) (b) Beam U-B6 (ρ_t=1.20%)

Figure 8. Load deflection response of beams U-B4 and U-B6 with and without stirrups

Load deflection response of UHPC beams U-B4 and U-B6 provided with stirrups were also evaluated utilizing the developed model and were compared to behavior of beams U-B4 and U-B6 without stirrups in Figure 8. It can be seen that eliminating stirrups did not affect performance of

theses beams in terms of load carrying capacity and ductility. This trend agrees with measured data in tests (Kodur et al., 2018) wherein beams U-B4 and U-B6, with no shear reinforcement reached their ultimate moment capacity under dominant shear loading. As can be observed, unlike NSC beams, eliminating stirrups did not lead to abrupt failure before yielding the reinforcing bars owing to high tensile strength of UHPC and bridging effect facilitated by steel fibers.

5. Conclusions

A numerical model is developed and validated against experimental data under different loading conditions for tracing structural response of UHPC beams. Results from this study show that:

- Although UHPC exhibits significantly different mechanical properties as compared to conventional concrete, concrete damage plasticity model available in ABAQUS can be utilized with adjusted parameters to represent the material behavior of UHPC for modeling structural response.
- Model predictions of tensile damage in UHPC using scalar damage parameter along with principal direction is an effective way of capturing crack propagation zone and direction as well as failure mode of the beams as observed in the experiments
- UHPC beams possess high shear resistance, even without any stirrups, due to high tensile strength of UHPC, combined with bridging effect, facilitated by presence of steel fibers and thus can be designed without shear reinforcement.

6. Acknowledgment

The authors wish to acknowledge the support of U.S. Airforce Research Laboratory (AFRL), Metna Company, and Michigan State University for undertaking this research. Any opinions, findings, conclusions, or recommendations expressed in this paper are those of the authors and not necessarily reflect the views of the sponsors.

7. References

ABAQUS. *Version 6.14 Documentation*. Providence (RI): Dassault systems simulia crop, 2014.

Ahmed Sbia, L. et al., "Enhancement of Ultrahigh Performance Concrete Material Properties with Carbon Nanofiber." *Advances in Civil Engineering*, vol. 2014, Aug. 2014, p. e854729.

Chen, L., and B. Graybeal., "Modeling Structural Performance of Second-Generation Ultrahigh-Performance Concrete Pi-Girders." *Journal of Bridge Engineering*, vol. 17, no. 4, 2011, pp. 634–43.

Empelmann, M. et al., "Improvement of the Post Fracture Behaviour of UHPC by Fibres." *Second International Symposium on Ultra High Performance Concrete*, 2008, p. 177.

Fehling, E. et al., "Design Relevant Properties of Hardened Ultra High Performance Concrete." *International Symposium on Ultra High Performance Concrete*, Vol. 1, 2004, pp. 327–38.

Graybeal, B., "Compressive Behavior of Ultra-High-Performance Fiber-Reinforced Concrete." *ACI Materials Journal*, vol. 104, no. 2, 2007, p. 146.

Graybeal, B., "Flexural Behavior of an Ultrahigh-Performance Concrete I-Girder." *Journal of Bridge Engineering*, vol. 13, no. 6, Nov. 2008, pp. 602–10.

Jendele, L., and J. Cervenka., "Finite Element Modelling of Reinforcement with Bond." *Computers & Structures*, vol. 84, no. 28, 2006, pp. 1780–91,

Kang, S. et al., "Tensile Fracture Properties of an Ultra High Performance Fiber Reinforced Concrete (UHPFRC) with Steel Fiber." *Composite Structures*, vol. 92, no. 1, Jan. 2010, pp. 61–71.

Kodur, V.K.R. et al., "Analysis of Flexural and Shear Resistance of Ultra High Performance Fiber Reinforced Concrete Beams without Stirrups." *Engineering Structures*, vol. 174, 2018, pp. 873–84.

Kodur, V.K.R., and A. Agrawal., "Effect of Temperature Induced Bond Degradation on Fire Response of Reinforced Concrete Beams." *Engineering Structures*, vol. 142, 2017, pp. 98–109.

Mahmud, G.H. et al., "Experimental and Numerical Studies of Size Effects of Ultra High Performance Steel Fibre Reinforced Concrete (UHPFRC) Beams." *Construction and Building Materials*, vol. 48, 2013, pp. 1027–34.

Singh, M. et al., "Experimental and Numerical Study of the Flexural Behaviour of Ultra-High Performance Fibre Reinforced Concrete Beams." *Construction and Building Materials*, vol. 138, 2017, pp. 12–25.

Solhmirzaei, R., and V.K.R. Kodur., "Structural Behavior of Ultra High Performance Concrete Beams without Stirrups." *Transportation Research Board 97th Annual Meeting*, 2018.

Tysmans, T. et al., "Finite Element Modelling of the Biaxial Behaviour of High-Performance Fibre-Reinforced Cement Composites (HPFRCC) Using Concrete Damaged Plasticity." *Finite Elements in Analysis and Design*, vol. 100, 2015, pp. 47–53.

Yang, I. H. et al., "Flexural Response Predictions for Ultra-High-Performance Fibre-Reinforced Concrete Beams." *Magazine of Concrete Research*, vol. 64, no. 2, 2011, pp. 113–127.

Yoo, D.Y. et al., "Material and Bond Properties of Ultra High Performance Fiber Reinforced Concrete with Micro Steel Fibers." *Composites Part B: Engineering*, vol. 58, Mar. 2014, pp. 122–33.

Yoo, D.Y., and Y.S. Yoon., "Structural Performance of Ultra-High-Performance Concrete Beams with Different Steel Fibers." *Engineering Structures*, vol. 102, Nov. 2015, pp. 409–23.